

INVESTIGATION OF TOLERANCES FOR THE
PARAMETERS OF THE PROPOSED LBL TEST-BED LINEAR INDUCTION ACCELERATOR

S. Chattopadhyay, A. Faltens, L. J. Laslett, and L. Smith
University of California Lawrence Berkeley Laboratory

I. INTRODUCTION

The Lawrence Berkeley Laboratory has proposed the construction of a Test-Bed linear induction accelerator¹⁾ to test the technique of accelerating heavy ions by use of induction modules and to investigate the transverse focusing of the ion beam by a FODO sequence of magnetic quadrupole lenses. The induction accelerator is intended to accept a 6- μ sec bunch of Cs^{+1} ions with 3-MeV kinetic energy ($\beta_0 \approx 0.007$) from a sequence of a few pulsed drift tubes and to accelerate these ions to a kinetic energy of approximately 25 MeV ($\beta \approx 0.020$) in a distance $\approx 10^2$ meter. The approximately 3-fold increase of velocity, combined with bunching of the beam by a factor of two, would result in a six-fold increase of current. A favorable value of transverse emittance -- e.g., $\pi \epsilon_N = (2.5 \times 10^{-5}) \pi$ meter radian, normalized -- then could be expected to permit a beam current that increases from $I_0 = 2.5$ A (≈ 15 μ C) to $I \approx 15$ A to be accommodated within an acceptable aperture.²⁾

To facilitate the investigation of tolerance limits that would be desirable to impose on the acceleration wave-forms -- and, more generally, to permit study of the expected dynamical behavior of beams of different quality and intensity -- we have constructed an illustrative schedule for the acceleration wave-forms and have prepared programs for the numerical examination of the consequences that could result from errors in wave-form magnitude, timing, or etc. and from variations in the initial characteristics of the beam. The design of appropriate wave-forms was initially undertaken by treating the longitudinal field $E(z,t)$ as a continuous function of z , but, with such work as a guide, impulsive wave-forms were then adopted for application at intervals (e.g., at 1-meter intervals) along the accelerator. A check of the uniformity of the linear charge density at various fixed times indicated that this transition to impulsive fields could be made successfully if the acceleration and bunching begin gradually. Considerations that entered into the wave-form design are summarized in Sect. II and some tolerance questions that warrant attention are discussed in Sect. III. The investigation of tolerance limits was begun only very shortly prior to the start of the Workshop (and continued to a limited degree during the Workshop); accordingly, although initial results appeared favorable, it clearly would be premature to report tolerance results at this time.

Following the acquisition of sufficient information concerning the tolerance restrictions for longitudinal acceleration, for

a satisfactory representative set of wave-forms, we are prepared to extend the computational work to a similar investigation of beam-envelope behavior in the FODO transport system of the accelerator. It is planned, for convenience, initially to consider this transport system to be strictly periodic spatially (occupancy factor, $\eta = 1/2$; half-period, $L = 1$ meter), although a final design of quadrupole lenses meriting subsequent examination well might divide the Test-Bed into two or three sections characterized by successively increasing values of L and certainly will require space for occasional pumping ports, etc. The work in progress does not take collective effects into account explicitly, but parameters controlling potential collective instabilities have been the subject of other theoretical and computational investigations.

II. THE LONGITUDINAL ACCELERATING FIELD

1. Specifications

Cs^{+1} to be accelerated from

$\beta_0 = 0.007$ to $\beta \approx 0.020$;

Little initial spread of β ;

Inject for an interval ≈ 6 μ sec;

Accelerate with spatial bunching by a factor ≈ 2 ;

Maintain the linear ion density substantially constant, vs. z , at every fixed t ;

Assume that one will subsequently design and provide "ears" to the applied wave-forms, to compensate for longitudinal space-charge forces at the ends of the bunch;

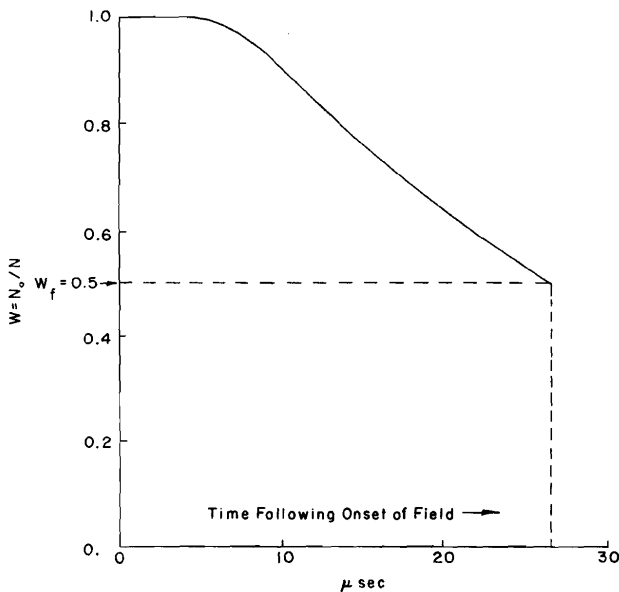
Conform to technological restrictions concerning the magnitude, shape, and volt-sec of the applied wave-forms (e.g., E less than circa 0.30 or 0.35 MV/m and $\phi \lesssim 0.8$ volt-sec).

The specification that the linear charge density along the bunch shall be constant at any fixed time is favorable with respect to avoidance of excessive transverse space-charge defocusing forces, and the avoidance of a significant $d\lambda/dz$ in the interior implies that the wave-forms require only the addition of modest corrective fields ("ears") at the ends in order to compensate for longitudinal space-charge forces.

2. Continuous Longitudinal Fields

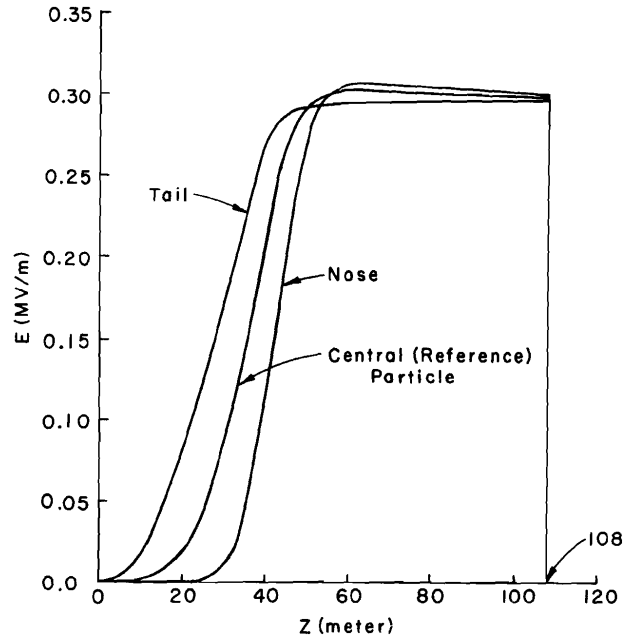
In the work that follows we make frequent use of "scaled" variables τ and F , where $\tau = ct$ and $E = \frac{A_1 \mu c^2}{q_e} F$. If the requirement that the longitudinal density remain constant along the beam (at fixed t) is to be maintained, it is clear that no particle should experience a longitudinal electric field until the entire beam is within the accelerator. Accordingly, if injection occurs within the interval $0 < \tau < 1800$, one may arrange that $E \neq 0$ only for $\tau > \tau_G$ where, for example, $\tau_G = 1850$. Subject to this restriction, one can prescribe the functional form of the field $F(z(\tau))$ acting on a reference particle (e.g., on a particle injected at the mid-point of the bunch) and also a function $w(\tau - \tau_G)$ that describes the factor by which the bunch length is shortened. The requisite wave-forms, $F(z, \tau)$, then may be derived (in practice, numerically) so that the desired constancy of $\lambda(z)$ is achieved -- Note 1.

An example of a selected bunching function, $w(\tau - \tau_G)$, is shown in Fig. 1. Figure 2 shows, also as an example, the form of the function $E(z(\tau))$ chosen in this initial work to represent the field acting on the reference particle, together with the corresponding fields acting on particles at the head and tail of the beam. In anticipation of the use of localized fields it has appeared desirable that the acceleration and bunching begin gradually -- most particularly if the constancy of linear density vs. z is to be maintained throughout the acceleration -- and the functions illustrated in Figs. 1 and 2 were designed with this intent. Subsequent to this gradual onset, the fields are permitted to grow comparatively rapidly to



XBL 801-7802

Fig. 1. An example of the bunching function, $w(\tau - \tau_G)$.



XBL 801-7796

Fig. 2. An example of the field on a reference particle, and of the associated fields on the nose and tail particles when the bunching function is that shown in Fig. 1.

attain values limited chiefly by technological considerations. There has been no attempt, in the work described here, however, to construct a fully optimized design, since the object of this work is an investigation of tolerances.³⁾

3. Discrete Impulsive Fields

Prior to the investigation of tolerances, the continuous longitudinal field (Sub-section 2) was discretized into a sequence of impulsive fields (nominally at 1-meter intervals). Values of F at each of the discrete z values were obtained at seven values of τ (within the interval during which the beam would be present) and the corresponding wave-forms were obtained as a least-squares fit to a polynomial of the form

$$F(\tau) = E_C + A_1 D + A_2 D^2 + A_3 D^3 + A_4 D^4,$$

where

$$D = \tau - A_0,$$

$$A_0 = \tau - A_{\text{Ref.}},$$

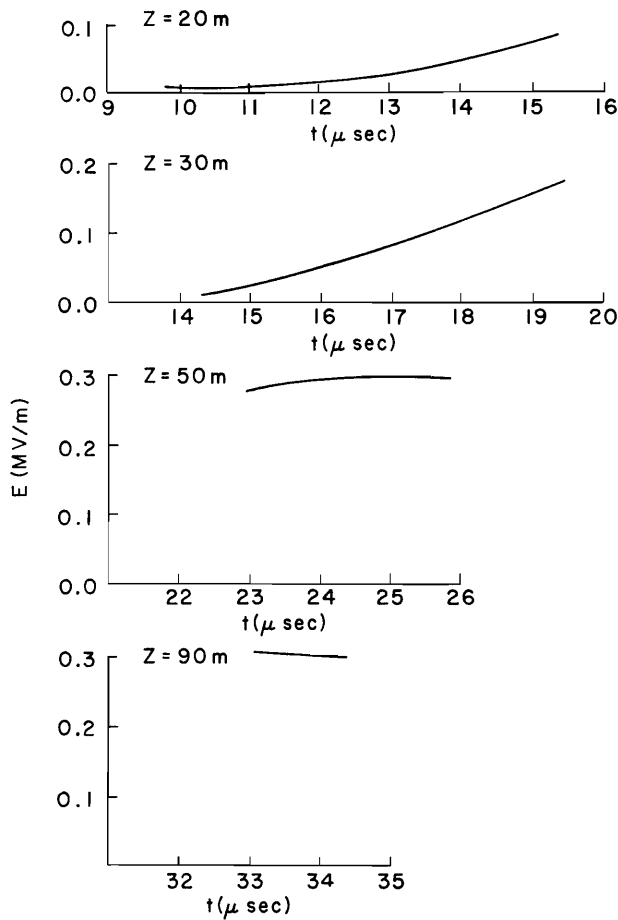
and

$$E_C = F(\tau_{\text{Ref.}}).$$

The parameters E_C and A_i ($i=0, \dots, 4$) are dimensioned variables, with each index value corresponding to a discrete z value, and are stored for subsequent use in other programs.

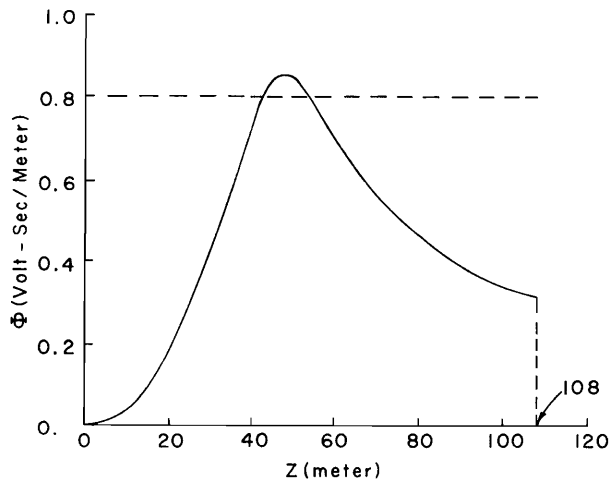
A few representative wave-forms, as given by such polynomials, are shown on Fig. 3 for the field sketched (prior to discretization) in

Fig. 2. The corresponding flux-changes per meter, $\int E dt$, are shown as a function of z on Fig. 4.



XBL 801-7800

Fig. 3. Representative wave-forms for the acceleration schedule of Figs. 1 and 2.



XBL 801-7797

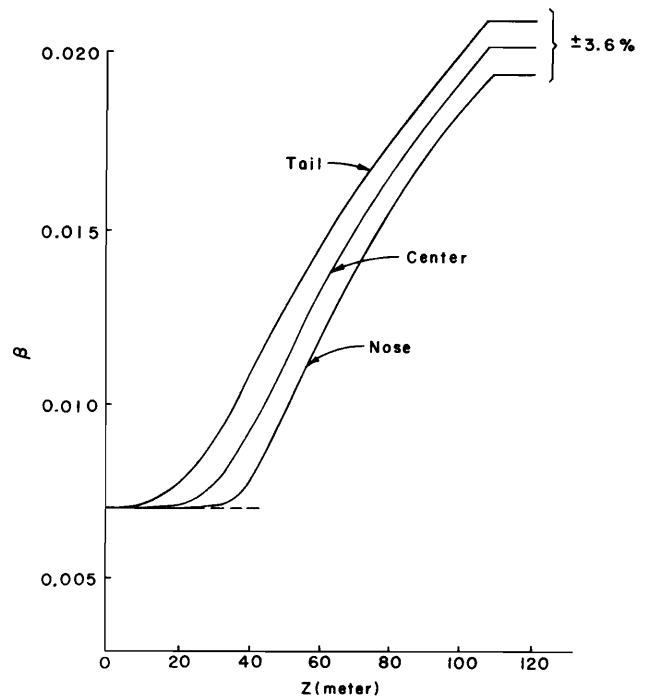
Fig. 4. The flux swing per meter for the acceleration fields of Figs. 1 and 2.

The longitudinal dynamics of particles moving under the action of a sequence of impulsive fields can be supplemented by evaluations of the local bunching (specifically of N_0/N), as indicated in Note 2, and the bunching appears to remain substantially constant with respect to z at fixed time. For the specific longitudinal field mentioned here, the resulting increase of β is as shown on Fig. 5 and the bunching is such that $N_0/N = 0.5$, implying an increase of current by a factor⁴) approximately $3/0.5 = 6$.

Although the incident beam is presumed to be composed of particles with substantially identical values of β_0 , phase plots (e.g., of β vs. z , at fixed time) can be constructed by performing computations for particles with somewhat different values of β_0 . The evolution of such phase plots, for an overall spread of β_0 much greater than would be expected in practice, is illustrated in Fig. 6. Corresponding plots of kinetic energy vs. t (at fixed z) are shown on Fig. 7.

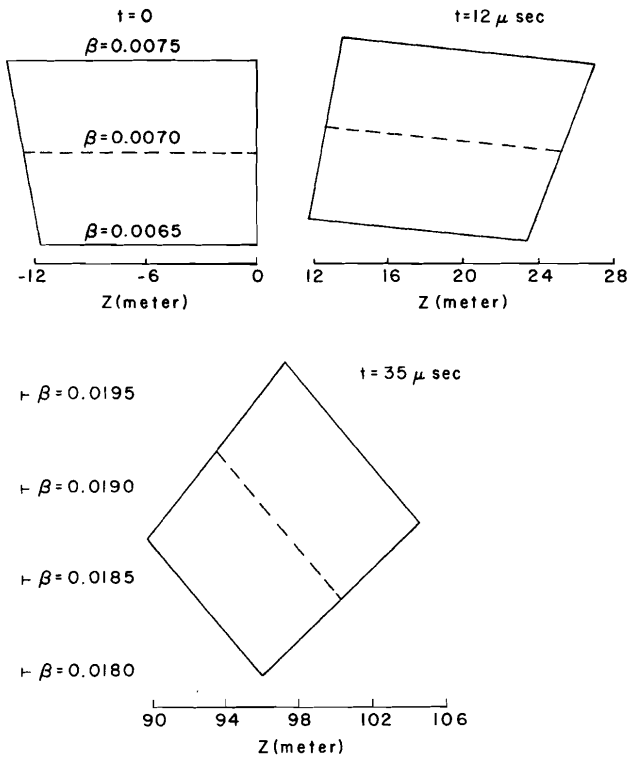
III. THE STUDY OF TOLERANCES

We have begun to investigate the sensitivity of the acceleration process to the complete or partial failure of one or more acceleration cavities -- with initial results that appear to be favorable. One effect that can result from failures of this type is illustrated in Fig. 8, from which one sees that the failure of a cavity may result in a particle quite near the tail of the beam drifting (as indicated by the broken dashed line) outside the region covered by the



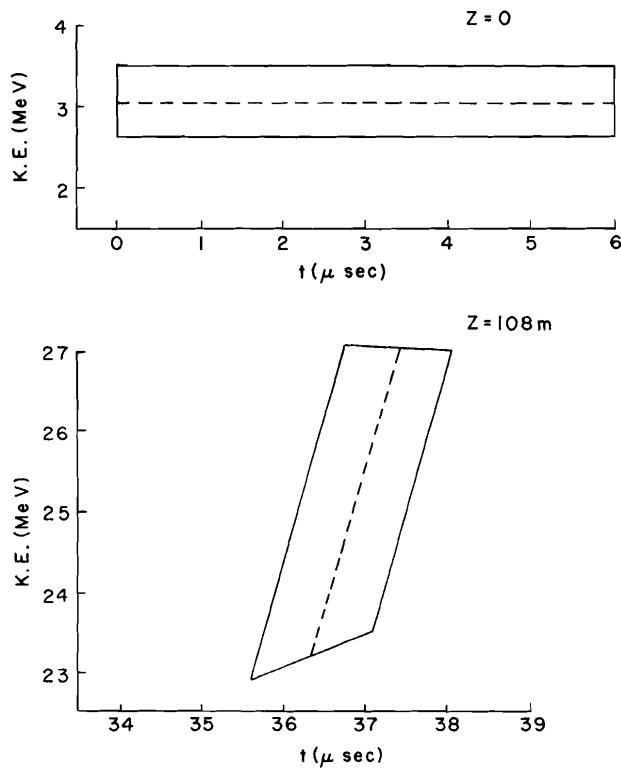
XBL 801-7804

Fig. 5. The growth of β , from an initial value $\beta_0 = 0.007$, for the fields of Figs. 1 and 2.



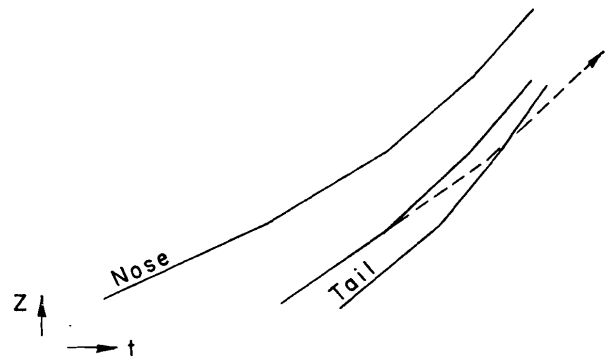
XBL 801-7801

Fig. 6. Evolution of phase diagrams, β vs. z at constant t , with the initial spread of β markedly greater than would be expected in practice.



XBL 801-7796

Fig. 7. Plots of kinetic energy vs. t , at constant z , for the case illustrated in Fig. 6.



XBL 801-7799

Fig. 8. An illustration of a possible effect, on a particle near the tail of the beam, of a cavity failure.

applied wave-forms (region bounded by the solid lines). A more detailed investigation of this and related effects (such as the response to timing errors, variations of β_0 , etc.) ultimately may require the extension of the wave-forms into regions where a field is not required under ideal conditions, in addition to the provision of some supplemental fields near the ends in order to compensate for longitudinal space-charge forces.

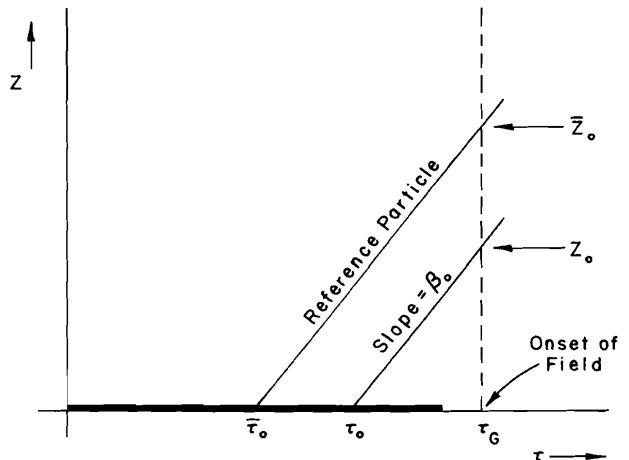
NOTES

Note 1. The Bunching Factor in the Case of Continuous Fields

Denoting the z and τ values for a reference ion by \bar{z} and $\bar{\tau}$, we specify $F(\bar{z})$ for the reference particle and have

$$d(z-\bar{z})/d\tau = \beta - \bar{\beta} \text{ and } d(\beta - \bar{\beta})/d\tau = F(z, \tau) - F(\bar{z}(\tau)).$$

With $w(\tau - \tau_G) [= N_0/N]$ also specified, we wish (for notation, see Fig. 9)



XBL 801-7803

Fig. 9. Illustration of notation employed in Note 1, leading to the relation $z - \bar{z} = (z - \bar{z})_0 \cdot w = \beta_0(\bar{\tau}_0 - \tau_0) \cdot w$.

$$\begin{aligned} z - \bar{z} &= (z - \bar{z})_0 \cdot w \\ &= \beta_0 (\bar{\tau}_0 - \tau_0) \cdot w, \end{aligned}$$

so that

$$\beta - \bar{\beta} = \beta_0 (\bar{\tau}_0 - \tau_0) \frac{dw}{d\tau}$$

$$\text{or } \beta = \bar{\beta} + \beta_0 (\bar{\tau}_0 - \tau_0) \frac{dw}{d\tau} \quad (N1)$$

and

$$\begin{aligned} F(z, \tau) - F(\bar{z}(\tau)) &= \beta_0 (\bar{\tau}_0 - \tau_0) \frac{d^2 w}{d\tau^2} \quad \text{or} \\ F(z, \tau) &= F(\bar{z}(\tau)) + \beta_0 (\bar{\tau}_0 - \tau_0) \frac{d^2 w}{d\tau^2}. \quad (N2) \end{aligned}$$

Equation (N2) thus provides the desired values of F for particles crossing the location z at time $\tau = ct$. The corresponding β is given by Eqn. (N1), or may be obtained by integration of $d\beta/d\tau = F$, while z is obtained from $dz/d\tau = \beta$. If, in practice, one integrates with respect to z (in order to obtain results at regularly spaced z values), one must interlace integrations with respect to τ in order to obtain the reference field $[F(\bar{z}(\tau))]$, required by Eqn. (N2) at values of τ common to the reference and trial particles.

If the function $F(z, \tau)$ is not specified through use of the bunching function $w(\tau - \tau_0)$, the local value of N_0/N may be evaluated for any explicit specification of F through introduction of auxiliary variables $u = [\partial\tau/\partial\tau_0]_{z=\text{const.}}$ and $v = \beta [\partial\beta/\partial\tau_0]_{z=\text{const.}}$ (with $u_0 = 1$, $v_0 = 0$). One then employs the coupled total differential equations

$$\left. \begin{aligned} \frac{d\tau}{dz} &= \frac{1}{\beta} \\ \frac{d\beta}{dz} &= \frac{F}{\beta} \\ \frac{du}{dz} &= -\frac{v}{\beta^3} \\ \frac{dv}{dz} &= u \frac{\partial F}{\partial \tau} \end{aligned} \right\} \text{or } \left\{ \begin{aligned} \frac{dz}{d\tau} &= \beta \\ \frac{d\beta}{d\tau} &= F \\ \frac{du}{d\tau} &= -\frac{v}{\beta^2} \\ \frac{dv}{d\tau} &= \beta u \frac{\partial F}{\partial \tau} \end{aligned} \right.$$

and computes the local density ratio as

$$N_0/N = \frac{\beta u}{\beta_0}. \quad \text{In the particular case that } F(z, \tau)$$

is given by Eqn. (N2), the ratio \ddot{w}/w (with dots denoting $d/d\tau$) is independent of z and may be identified with $\partial F/\partial z$. With β and w initially zero, the auxiliary variables u and v then will be

$$u = (\beta_0/\beta)w \quad \text{and} \quad v = \beta_0 \dot{\beta} w - \beta_0 \beta \dot{w},$$

$$\text{with } \frac{1}{\beta u} \frac{dv}{d\tau} = \ddot{\beta} - \beta \ddot{w}/w = dF/d\tau$$

$$= dF/d\tau - \beta \partial F/\partial z = \partial F/\partial \tau, \quad \text{as required.}$$

Note 2. The Bunching Factor in the Case of Impulsive Fields.

A(i). Between cavities:

$$\Delta\tau = \frac{1}{\beta} \Delta z, \quad \text{i.e., } \tau_{n+1} = \tau_n + \frac{1}{\beta_n} (z_{n+1} - z_n),$$

while β remains unchanged.

(ii). Traversing a cavity:

τ is unchanged,

and

$$\beta_{n+1} = \sqrt{\beta_n^2 + 2F_{n+1}}.$$

B. For infinitesimally neighboring trajectories ($D\tau$ and $D\beta$):

(i). In passing from one cavity to the next:

From Fig. 10,

$$\frac{\delta z_n}{\delta z_{n+1}} = \frac{[(\beta_n + \beta_{n-1}) - (D\beta_n - D\beta_{n-1})]D\tau_n}{[(\beta_{n+1} + \beta_n) - (D\beta_{n+1} - D\beta_n)]D\tau_{n+1}}$$

is a factor that may be applied to convert the old density ratio (initially unity, at $z = 0$) to the new density ratio, where

$$D\tau_{n+1} = D\tau_n - \frac{D\beta_n}{\beta_n} \Delta z$$

and

$$D\beta_{n+1} \approx \frac{\beta_n D\beta_n + (\partial F_{n+1}/\partial \tau) D\tau_{n+1}}{\beta_{n+1}}.$$

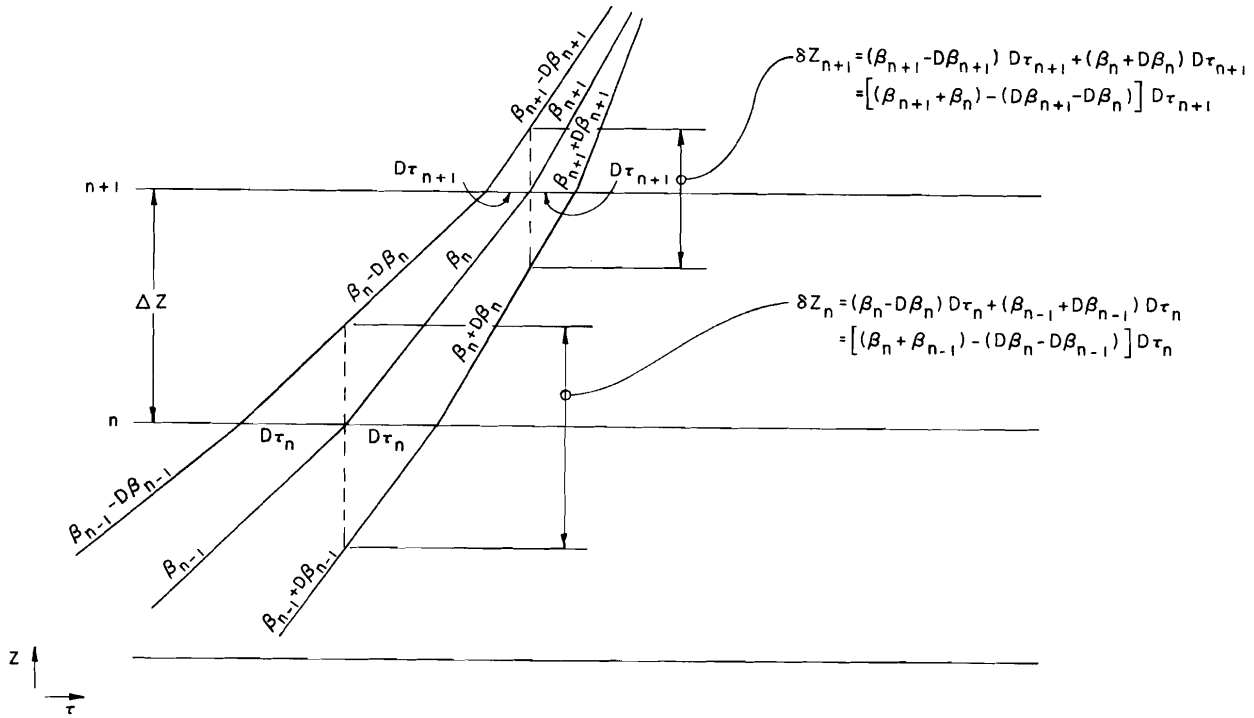
(ii). In moving between two cavities:

To update linear ion density (N) between cavities ($\delta z < \Delta z$), one recalls that, from B(i) above (with $n+1$ replaced by n), one employs a denominator $\delta z_n = [(\beta_n + \beta_{n-1}) - (D\beta_n - D\beta_{n-1})]D\tau_n$ in evaluating $\delta z_{n-1}/\delta z_n$. From Fig. 11 it is evident that to obtain the density ratio at a point between z_n and z_{n+1} one should replace δz_n by $s_U + s_L$ — i.e., the density factor at $z = z_n$ should be corrected by the factor

$$\frac{\delta z_n}{s_U + s_L} = \frac{\text{denominator}}{2[\beta_n D\tau_n - (\delta z/\beta_n) D\beta_n]}$$

to obtain the ratio at $z = z_n + \delta z$.

In practice the infinitesimal quantities $D\tau$ and $D\beta$ may be initialized to 1 and 0, respectively, since only their relative values are of significance.

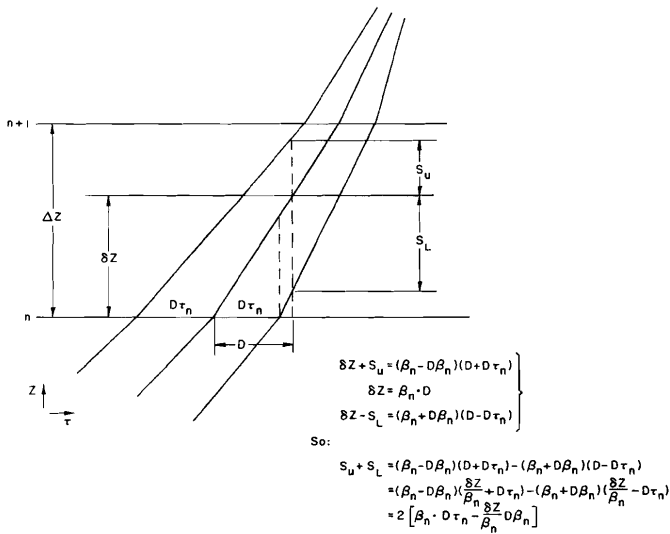


XBL 801-7806

Fig. 10. Kinematics relevant to the change of particle density in passing from one cavity to the next.

REFERENCES AND NOTES

1. See presentation by A. Faltens -- this Workshop. See also LBL Report PUB-5031 (September 1979) and earlier LBL Report HIFAN-67 (16 January 1979).
2. Experiments now in progress at the Lawrence Berkeley Laboratory are directed to a study of the optical characteristics of a contact-ionization Cs⁺¹ source.
3. In a separate investigation, to which we have returned following the Workshop, further consideration is being given to the specification of wave-forms and lattice structures that may prove to be significantly more economical than those mentioned in the present report.
4. The acceleration and bunching produced by the fields described by Figs. 1-3, and by similar field systems³⁾ to which we have given consideration, results in a current that increases slightly less rapidly than in direct proportion to the kinetic energy. Such current increases permit the transport of a non-relativistic Kapchinskij-Vladimirskij beam through a periodic focusing system of constant K and η without the space-charge tune depression during the course of acceleration becoming more pronounced than initially (for the reference particle).



XBL 801-7805

Fig. 11. Kinematics relevant to the change of particle density in passing between induction cavities.